Supplemental Experimental Procedures and Figures:

Genotyping:

Genomic DNA was prepared from tail biopsy using DirectPCR Lysis Reagent (Viagen Biotech, Inc., Los Angeles, CA) and subjected to PCR amplification using specific sets of PCR primers for each genotype, including LRRK2 WT and G2019S transgenic mice (LRRK2-F: TATTGGGCTACAACCGGAAA and LRRK2-prp R: CTCCATCAAAGGGACCTGAA), α-synuclein WT and A53T transgenic mice (PrpEx2-F: TACTGCTCCATTTTGCGTGA and SNCA-R: TCCAGAATTCCTTCCTGTGG), and *LRRK2*$^{-/-}$ mice (LRRK2 Ex1F2: AGGAGGAGGAGGCTCTGAAG and LRRK2-Intron 2R: GGCATTCGGGAAACATCACT).

Quantitative reverse transcriptase-PCR (Q-RT-PCR) assay:

Brains of *nTg* control and different transgenic strains were quickly dissected out and frozen vt dry ice. Total RNA was isolated from frozen tissues with TRYZOL reagent (Invitrogen) and cDNA was synthesized from 1ug of RNA by First strand kit (SuperArray Bioscience Corporation). SYBR Green real-time PCR detection method was utilized in the presence of human LRRK2 specific primers (5'-GAGGCGCTTCGAGCTATTT-3' and 5'-CTGAATCCCAGGATTTCCAA-3'), or primers in the region common for human and mouse LRRK2 (5'-AGCAGGACAAAGCCAGCCTCA-3' and 5'-GATGGCAGCATTGGGATACAG-3'). The amplification of PCR reaction was normalized by β-actin expression (5'-CGTTGACATCCGTAAAGACC-3' and 5'-GCTAGGAGCCAGAGCAGTAA-3').

Behavior Tests

Rotarod test: as described previously (Chandran et al., 2007), mice were placed onto a rotating rod with auto acceleration from 0 rpm to 40 rpm for 1 min (San Diego Instruments, San Diego, CA). The length of time the mouse stayed on the rotating rod was recorded.

Open-field test: as described previously (Chandran et al., 2007), the ambulatory and rearing activities of mice were measured by the Flex-Field activity system (San Diego Instruments, CA). Flex-Field software was used to trace and quantify mouse movement in the unit as the number of beam breaks per 30 min.

Immunohistochemistry and Light Microscopy

As described previously (Cai et al., 2005), mice were perfused via cardiac infusion with 4% paraformaldehyde in cold PBS. To obtain frozen sections, brain tissues were removed and submerged in 30% sucrose for 24 h and sectioned at 40 μm thickness with cryostat (Leica CM1950). Antibodies specific to glial fibrillary acidic protein (GFAP) (1:400, Sigma-Aldrich USA, St. Louis, MO), ionized calcium binding adaptor molecule-1 (Iba1) (1:500, Wako Chemicals USA, Richmond, VA), tryosine hydroxylase (TH) (1:1000, Pel-Freez Biologicals, Rogers, AR), HA (1:500, Santa Cruz Biotech, Santa Cruz, CA), α-syn (C20, 1:1000, Santa Cruz Biotech, Santa Cruz, CA), MTCOI (1:500, Invitrogen), cleaved caspase 3 (1:500, Cell Signaling, Danvers, MA), ubiquitin (1:2000, DAKO, Denmark), GM130 (1:500, BD), GM160 (1:2000, Sigma), Ctip2 (1:300, Abcam), βIII-tubulin (Chemicon) and NeuN (1:500, Millipore) were used as suggested by manufacturers. Alexa 488 or Alexa 568-conjugated secondary antibody (1:500, Invitrogen) was used to visualize the staining.

Electron Microscopy

Mice were perfusion fixed by a method designed to reduce morphological damage to metabolically sensitive structures (like mitochondria) in the mouse brain (Tao-Cheng et al., 2007). Briefly, the mouse was initially anesthetized in a plastic flow chamber with 5% isoflurane carried by 100% oxygen. After the mouse was unresponsive to toe pinch, it was moved to a perfusion station inside a chemical fume hood. Anesthesia was maintained by delivering 2% isoflurane in oxygen through a facemask. The chest cavity was opened, the heart was rapidly exposed, the right atrium was cut then a cannula inserted and clamped into the left ventricle. The fixative was then directly perfused into the ventricle (within 100 seconds of opening of the diaphram and within 20 seconds of cutting the right atrium). The fixative (a mixture of 2% gluteraldehyde and 2% paraformaldehyde in 0.1 N sodium cacodylate buffer, pH 7.4) was delivered by a controlled pressure device (Perfusion One by My Neuroscience) at a hydrostatic pressure of 150 mm Hg.

After perfusion fixation, brains were removed and vibratome-sectioned into 100 μm slices, and further immersion fixed in 4% glutaraldehyde from overnight to 2 wks. Slices were treated with 1% OsO_4 in cacodylate buffer for 1 hr on ice, and 0.25% uranyl acetate in acetate buffer at pH 5.0 overnight at 4 ˚C, dehydrated with ethanol and propylene oxide, and flat-embedded in epoxy resin between two plastic slides. The samples were then sectioned and examined on a JEOL electron microscope.

MitoSox Red Labeling

MitoSox Red (Molecular Probes, Invitrogen) Labeling was performed to evaluate the presence of superoxide within mitochondrial matrix (Mallajosyula et al., 2008). 200 μl of 0.9% sterile saline containing 10 μg of MitoSox was injected intravenously via the tail vein into 1-month old *nTg*,

G2019S, *A53T* and *A53T/G2019S* mice. Three or more mice per genotype were used in this study. Mice were sacrificed 90 minutes later. Brains were rapidly dissected out and fixed in cold 4% paraformaldehyde overnight, and sectioned at 40 μm by cryostat. MitoSox Red accumulation in the striatum was examined under confocal microscope (LSM510) and procured using LSM software.

Measurement of α-syn in Cerebrospinal Fluid by ELISA

Cerebrospinal fluid (CSF) was collected as described previously (Fleming et al., 1983). Briefly, mice were anesthestized and perfused transcardically with 30 ml of PBS (pH 7.4). 5-10 μl/mouse of CSF was collected by micro-volume syringes (Hamilton, Nevada) from the cisterna magna. Concentration of α-syn in the CSF was measured by Human α-syn ELISA kit (Invitrogen: KHB0061) following the manufacturer's instructions.

Tissue fractionation and Western blot

Brain tissues were homogenized with 10 volumes of sucrose buffer (0.32 M sucrose, 1 mM $NaHCO_3$, 1 mM $MgCl_2$, and 0.5 mM $CaCl_2$, plus protease and phosphatase inhibitor cocktails) and centrifuged at 1,000g for 10 min to separate supernatant (S1) and pellet (P1). Proteins concentrations in S1 were measured by BCA. S1 contains total α-syn protein, representing the sucrose fraction. An aliquot of S1 was diluted in the same volume of Triton-X100 extraction buffer (2% Triton-X100, 20 mM HEPES, plus protease and phosphatase inhibitor cocktails), homogenized by sonication, and centrifuged at 20, 000 × g for 30 min to obtain the Triton-X100-soluble (TX-sol) supernatant (S2) and Triton-X100-insoluble (TX-insol) pellet (P2). P2 was washed 4 times by 1% Triton-X100 buffer and centrifuged at 20, 000 × g for 10 min. The pellet

fraction was further extracted in 4% SDS buffer (4% SDS, 20 mM HEPES, plus protease and phosphatase inhibitor cocktail) by sonication and centrifuged at 20, 800 × g for 5 min. The supernatant (S3) were present as Triton-X100-insoluble (TX-insol) or SDS-soluble fraction. Proteins were size-fractioned by 4–12% NuPage BisTris-polyacrylamide gel electrophoresis (Invitrogen) using MOPS running buffer (Invitrogen), and transferred to polyvinylidene difluoride (PVDF) membranes. Antibodies specific to human/mouse α-syn (1:1000, Santa Cruz), phosphor (Ser 129)-α-syn (1:1000 diluting in 5% BSA, Wako), HA (1: 2000, Roche), and β-actin (1:3000, Sigma) were used in this study. Signals were visualized by enhanced chemiluminescence development (Pierce, Rockford, IL) and quantified on a Scion Image System (Frederick, MD).

Supplementary Figure Legends

Figure S1 Over-expression of human *LRRK2* in *LRRK2WT, G2019S*, and KD mice

(A) Western blot analysis shows LRRK2 expression in the brain of 1 month-old *nTg, G2019S* transgenic lines (E3, F7 and C3), and *WT LRRK2* transgenic lines (C77, C59, C74, C65, and C73) using a LRRK2 C-terminal antibody. Actin was used as the loading control.

(B) Western blot shows the expression of LRRK2 (upper panel) and α-syn (bottom panel) in a series of diluted whole brain homogenates from *nTg*, *G2019S*, *LRRK2WT*, *A53T* mice at 1 month of age. The sample was diluted from 2 to 32-fold for LRRK2, and 2 to 256-fold for α-syn. Actin was used as the loading control.

(C) In the upper panel, Western blot analysis shows the expression of HA-tagged human LRRK2 in the brain of 1 month-old *nTg*, *LRRK2WT-L, KD, LRRK2*$^{-/-}$, *LRRK2WT,* and *G2019S* mice using an HA antibody. Less samples of *LRRK2WT*and *G2019S* brain homogenates were loaded.

In the bottom panel, Western blot shows the expression of HA-tagged human LRRK2 in the brain of *LRRK2WT-L* and *KD*, as well as in a series of diluted whole brain homogenates from *LRRK2WT* mice at 1 month of age using an HA antibody. The sample was diluted from 2 to 16-fold. Actin was used as the loading control.

(D) Bar graph depicts the expression of *LRRK2* mRNA in the brain of *KD* and *LRRK2WT-L* transgenic mice analyzed by qRT-PCR. Data are showed as the relative expression fold to the endogenous *LRRK2* in the brain of *nTg* mice.

(E) A representative image shows the distribution of H2Bj-GFP (a GFP fusion protein located in the nucleus) in the brain of *tetO-H2Bj-GFP/CaMKII-tTA* double transgenic mice at 1 month of age. Ob: olfactory bulb; Cx: cortex; St: Striatum; Hip: hippocampus. Scale bar: 100 μm

(F) A representative image displays the distribution of H2Bj-GFP fusion protein in the substantia nigra pars compacta (SNc). DA neurons were labeled by TH staining (red). Under the *CaMKII* promoter, only a small fraction of DA neurons expressed H2Bj-GFP (arrows) in the midbrain. Scale bar: 100 μm.

(G) A representative image shows a few DA neurons expressing GFP under a high magnification. Scale bar: 20 μm.

Figure S2 Behavioral characterization of *LRRK2* WT and G2019S and *α-syn* A53T transgenic mice

(A-D) *G2019S* and *A53T* transgenic and control mice were weighted monthly (A-B). Rotarod test was used to examine the motor coordination and balance of *G2019S* and *A53T* transgenic and control mice (C-D). N >=10 per genotype. Data are presented as Means ± SEM. ***P <0.001.

(E-H) Littermate *nTg* (n = 10) and *LRRK2WT* (n = 11) mice were weighted monthly (E). Rotarod (F) and Open-field tests (G, H) were performed to examine the motor function of transgenic mice at 2 and 6 months of age. Data are presented as Means ± SEM. **p<0.05

(I-L) Representative images show Jade C (I), cleaved caspase3 (J), GFAP (K) and Iba1 (L) staining in the striatum of *LRRK2WT* mice at 12 months of age. N >= 3 per genotype. Scale bars: 50 μm (I, J, L); 100 μm (K).

Figure S3 Degeneration of medium size spiny neurons in the striatum of *A53T/G2019S* mice at 1 month of age

(A-C) Representative images show co-staining of cleaved-caspase3 (green, arrowhead) and Ctip2 (red) in the striatum of *A53T/G2019S* mice. Scale bar: 10 μm.

Figure S4 No exacerbation of α-syn-mediated neuropathology in *A53T/D1-GFP* double transgenic mice

(A-B) Representative images show GFAP-positive astrocytes in the striatum of one month-old *A53T* mice (A) and littermate *A53T/D1-GFP* double transgenic mice (B). Scale Bar: 100 μm.

(C-D) Representative images show microglia staining in the striatum of *A53T* transgenic mice at one month of age (C) compared to littermates *A53T/D1-GFP* mice (D). Scale bar: 20 μm.

Figure S5 *LRRK2* G2019S mutation does not accelerate *APP*-mediated neuropathology

(A-B) Representative images show reactive astrocytosis (A) in the striatum of *APP* inducible transgenic mice (Jankowsky et al., 2005) at 1 month of age as compared to littermate *APP/G2019S* double transgenic mice (B). Scale bar: 100 μm (A-B)

(C-D) Representative images show microglia (C) in the striatum of *APP* inducible transgenic mice at 1 month of age as compared to littermate *APP/G2019S* double transgenic mice (D). Scale bar: 10 μm (C-D).

Figure S6 G2019S *LRRK2* promotes the somatic accumulation of WT α-syn in the soma of striatal neurons of *α-synWT/G2019S* double transgenic mice

(A-D) Representative images show α-syn staining (green) in striatal neurons of 20-month old *G2019S* (A), 1-month old *α-synWT* (B), and *α-synWT /G2019S* mice (C, D). Human LRRK2 was stained with an anti-HA antibody (red, D). Nuclei were stained with Topro 3 (blue). N >= 3 per genotype. Scale bar: 10 μm.

Figure S7 α-syn and LRRK2 cause synergistic damage to Golgi apparatus in neurons of 6-month old mice.

(A-I) Representative images show GM130 staining (arrows, green) in the striatum of *nTg* (A), *LRRK2WT* (B), *G2019S* (C), *A53T* (D, G), *A53T/LRRK2WT* (E, H) and *A53T/G2019S* (F, I) mice at 6 months of age. Co-staining of GM130 (green) and α-syn (red) was shown in the striatum of *A53T* (G), *A53T/LRRK2WT* (H) and *A53T/G2019S* (I) mice. Neurons displaying somatic accumulation of α-syn were marked with asterisks. Normal GM130 staining was pointed by arrows in neurons. Nuclei were labeled by Topro 3 staining (blue). N >= 3 per genotype. Scale bar: 10 μm

(J) Bar graph quantifies the morphological changes of cis-Golgi in neurons of *LRRK2* and *α-syn* A53T transgenic mice at 6 months of age (> 300 neurons and ≥ 3 mice per genotype). Data are presented as Means ± SEM. *$p < 0.05$. #$p < 0.0005$

Figure S8 Over-expression of *LRRK2* impairs the dynamics of microtubules in neurons of 6-month old mice.

(A-C) Representative images show βIII tubulin (green) and HA (red) staining in the striatum of *LRRK2WT* (Aa, Ba, and Ca), *G2019S* (Ab, Bb, and Cb), *A53T/LRRK2WT* (Ac, Bc, and Cc) and *A53T/G2019S* (Ad, Bd, and Cd) mice at 6 month of age. Nuclei were labeled by Topro 3 staining (blue). N >= 3 per genotype. Scale bar: 10 μm.

(D-F) Representative images show βIII tubulin (green) and α-syn (red) staining in the striatum of *nTg* (Da, Ea, and Fa), *A53T* (Db, Eb, and Fb), *A53T/LRRK2WT* (Dc, Ec, and Fc) and *A53T/G2019S* (Dd, Ed, and Fd) mice at 6 month of age. The abnormal somatic accumulation of α-syn and βIII tubulin was marked by arrowheads. Nuclei were labeled by Topro 3 staining (blue). N >= 3 per genotype. Scale bar: 10 μm.

(G) Western blots of β-tubulin in RAB buffer-soluble supernatant (RAB-S) fraction of brain homogenates from *nTg* and *A53T/G2019S* transgenic mice at 6 month of age.

Figure S9 The expression of βIII-tubulin in the brain of *A53T, LRRK2WT* and *G2019S* transgenic mice

(A) Western blot analyses of total β-tubulin expression in *A53T* transgenic mice at 1 and 12 months of age. The expression of β-actin was used as loading control.

(B) Western blot shows total β-tubulin expression in *LRRK2WT, G2019S, and A53T/LRRK2WT* transgenic mice at 6 and 24 months of age. The expression of β-actin was used as loading control.

Figure S10 Abnormal mitochondria from striatal neurons of *A53T*, *A53T/LRRK2WT*, and *A53T/G2019S* double transgenic mice

(A-D) Representative images show mitochondria (red, MTCOI staining) in striatal neurons of *G2019S* (A), *A53T* (B), *A53T/WT* (C), and *A53T/G2019S* (D) transgenic mice. Nuclei were labeled by Topro 3 (blue). Enlarged mitochondria were marked by arrows. Scale bar: 10μm. N = 3 per genotype.

Figure S11 Generation of *LRRK2*$^{-/-}$ mice

(A) Schematic sketch outlines the deletion of the 2nd coding exon of *LRRK2* by the *Cre-LoxP* system.

(B) The homologous recombination of *LRRK2* targeting vector at *LRRK2* locus was verified by Southern blot. As expected, a new 4.4 kb *SphI* fragment was detected from the mutant allele in addition to the 12.3 kb *SphI* fragment generated from the wild-type allele. (C) The deletion of exon 2 in *LRRK2* KO mice was revealed by PCR using a pair of PCR primers flanking exon 2. (D) Western blot analysis showed LRRK2 expression in wild-type (+/+), heterozygous knockout (+/-) and homozygous knockout (-/-) mouse brains using the antibody JH5514 against the C-terminal region of LRRK2.

Figure S12 Characterization of *LRRK2*$^{-/-}$ mice

(A) Line graph shows the body weight of *LRRK2*$^{-/-}$ mice compared with littermate *LRRK2*$^{+/+}$ and *LRRK2*$^{+/-}$ mice (A, n = 10 per genotype).

(B) Line graph shows the results of Rotarod test of *LRRK2*$^{-/-}$ mice.

(C-D) Line graphs depict the results of open-filed test on ambulatory (C) and rearing (D) activities of *LRRK2*$^{-/-}$ mice as compared to control mice.

(E-H) Representative images show GFAP (E-F) and Iba1 staining (G-H) in the striatum of *LRRK2*$^{-/-}$ and littermate control mice at 20 months. Activated microglia was pointed by arrowheads. Scale bars 200 μm (E, F), 20 μm (G, H).

Figure S13 Inhibition of *LRRK2* expression delays the progression of α-syn-mediated neuropathology, and reduces the somatic accumulation and aggregation of α-syn.

(A-F) Representative images show GFAP (green), Iba1 (green), and α-syn (green) staining in the striatum of *A53T/LRRK2*$^{+/+}$ (A, C, E) and age-matched *A53T/LRRK2*$^{-/-}$ (B, D, F) at 6 months of age. Activated microglia and somatic accumulation of α-syn were marked by arrows. Nuclei were labeled by Topro 3 staining (blue). Scale bars 100 μm (A, B), 20 μm (C, D), 10 μm (E, F). N = 3 per genotype.

(G) Bar graph depicts the numbers of GFAP-positive cells in the dorsal striatum of *A53T/LRRK2*$^{+/+}$ and age-matched *A53T/LRRK2*$^{-/-}$ at 6 months of age using unbiased stereological methods. N = 3 per genotype. Data are presented as means ± SEM. *$p<0.05$.

(H) Western blot shows α-syn detected in the TX-insoluble fraction of brain homogenates from 6 month-old *A53T/LRRK2*$^{-/-}$ mice as compared to age-matched *A53T*/*LRRK2*$^{+/+}$ mice.

Figure S1

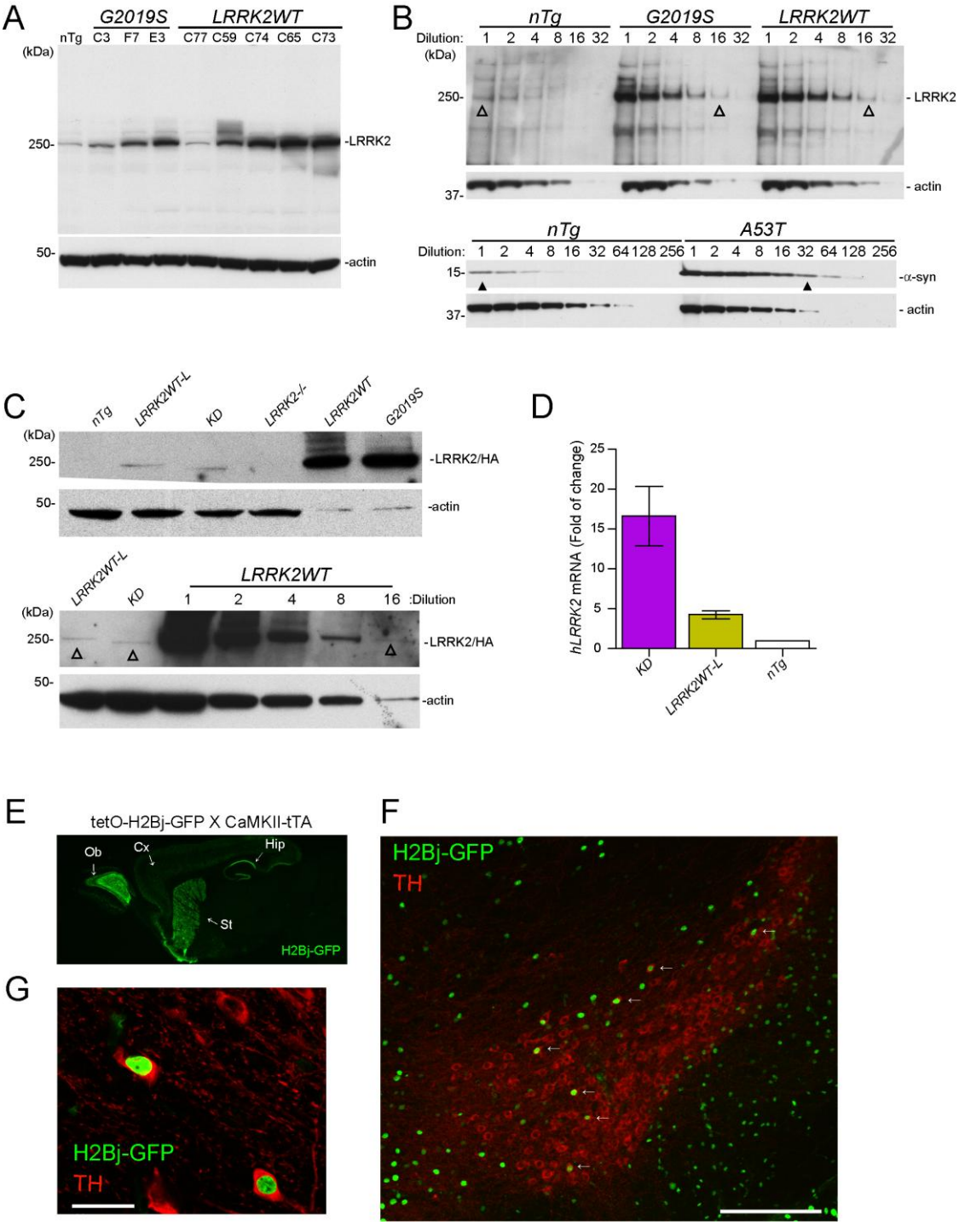
A
G2019S
LRRK2WT
nTg C3 F7 E3 C77 C59 C74 C65 C73
(kDa)
250-
-LRRK2
50-
-actin
B
nTg
G2019S
LRRK2WT
Dilution: 1 2 4 8 16 32 1 2 4 8 16 32 1 2 4 8 16 32
(kDa)
250-
- LRRK2
37-
- actin
nTg
A53T
Dilution: 1 2 4 8 16 32 64 128 256 1 2 4 8 16 32 64 128 256
15-
-α-syn
37-
- actin
C
nTg
LRRK2WT-L
KD
LRRK2-/-
LRRK2WT
G2019S
(kDa)
250-
-LRRK2/HA
50-
-actin
LRRK2WT-L
KD
LRRK2WT
1 2 4 8 16 :Dilution
(kDa)
250-
-LRRK2/HA
50-
-actin
D
hLRRK2 mRNA (Fold of change)
25
20
15
10
5
0
KD
LRRK2WT-L
nTg
E
tetO-H2Bj-GFP X CaMKII-tTA
Ob
Cx
Hip
St
H2Bj-GFP
F
H2Bj-GFP
TH
G
H2Bj-GFP
TH

Figure S2

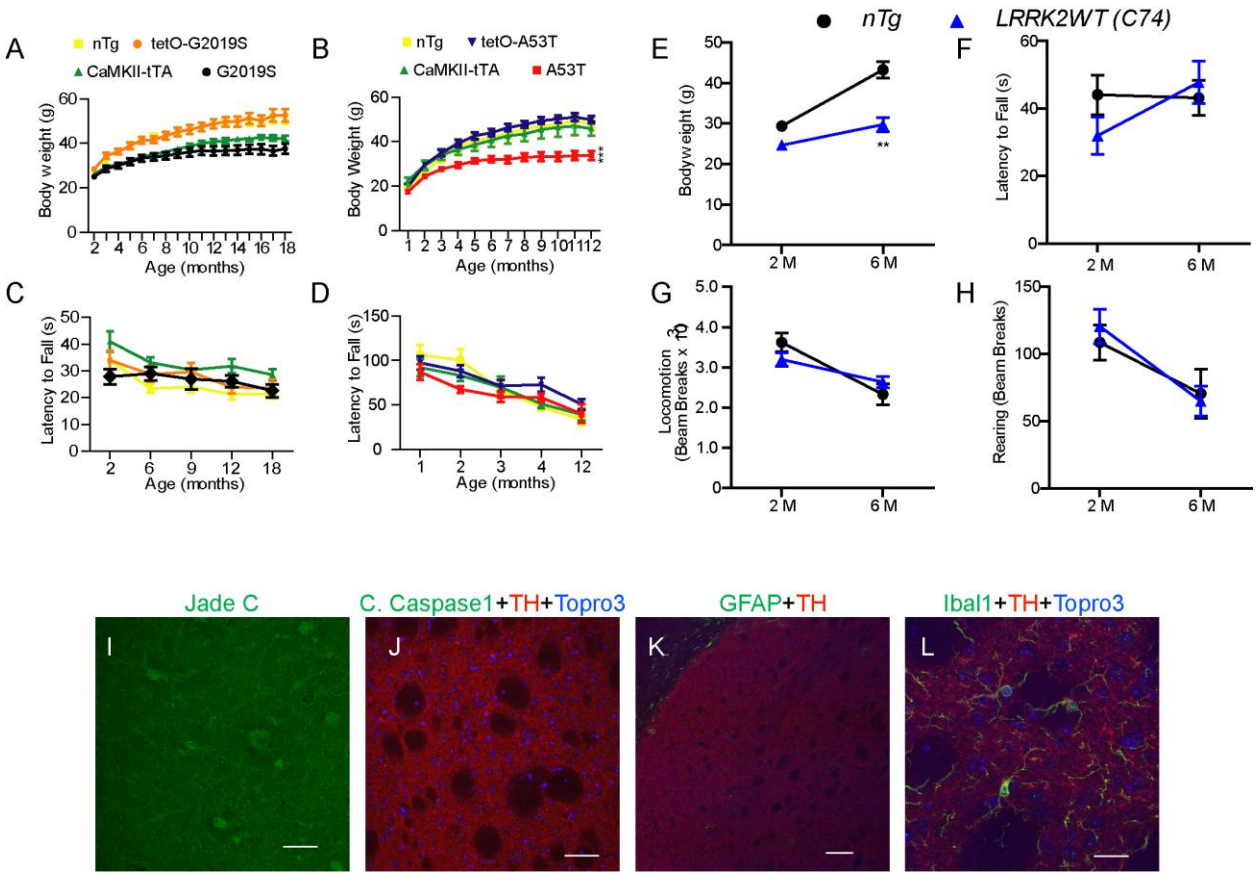
A
nTg
tetO-G2019S
CaMKII-tTA
G2019S
Body weight (g)
Age (months)
B
nTg
tetO-A53T
CaMKII-tTA
A53T
Body Weight (g)
Age (months)
C
Latency to Fall (s)
Age (months)
D
Latency to Fall (s)
Age (months)
E
nTg
LRRK2WT (C74)
Bodyweight (g)
2 M
6 M
F
Latency to Fall (s)
2 M
6 M
G
Locomotion (Beam Breaks x 10^2)
2 M
6 M
H
Rearing (Beam Breaks)
2 M
6 M

Jade C
I
C. Caspase1+TH+Topro3
J
GFAP+TH
K
Iba1+TH+Topro3
L

Figure S3

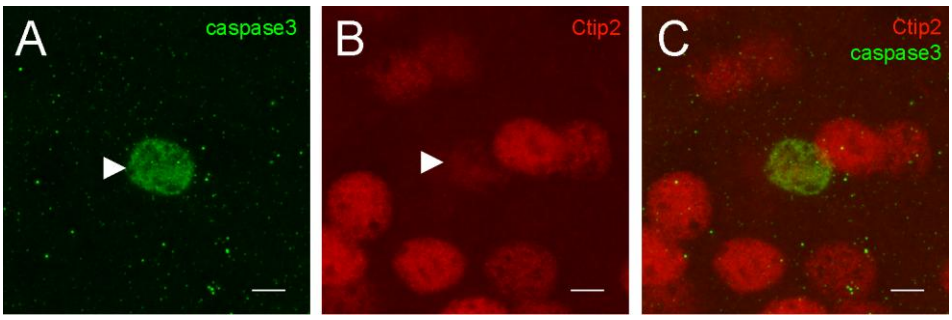

Figure S4

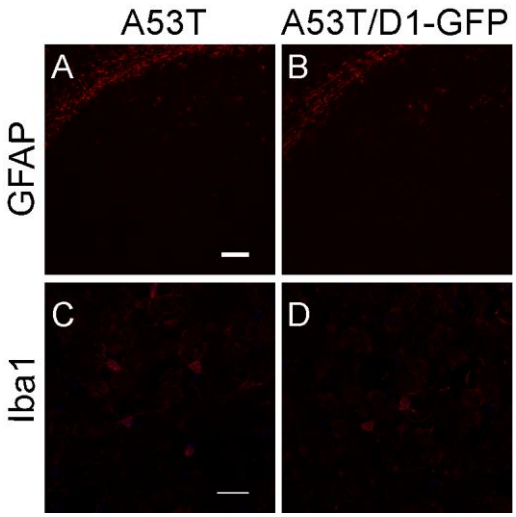

Figure S5

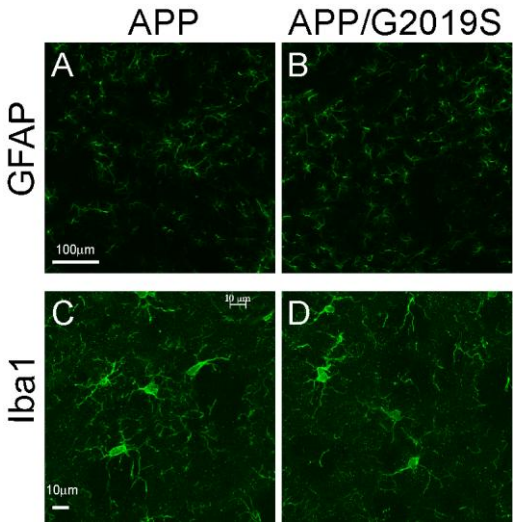

Figure S6

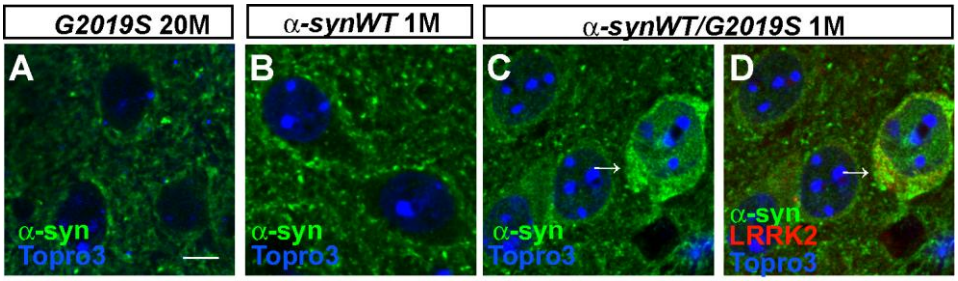

Figure S7

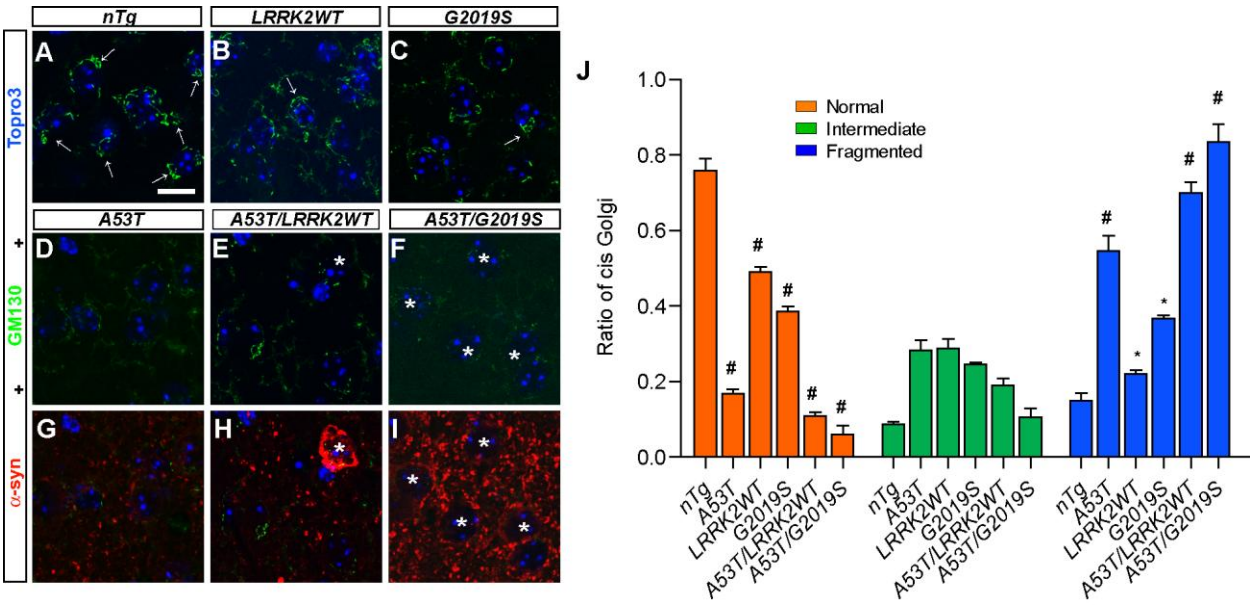
nTg
LRRK2WT
G2019S
A53T
A53T/LRRK2WT
A53T/G2019S
Topro3
GM130
α-syn
A
B
C
D
E
F
G
H
I
J
Ratio of cis Golgi
Normal
Intermediate
Fragmented
1.0
0.8
0.6
0.4
0.2
0.0
nTg
A53T
LRRK2WT
G2019S
A53T/LRRK2WT
A53T/G2019S

Figure S8

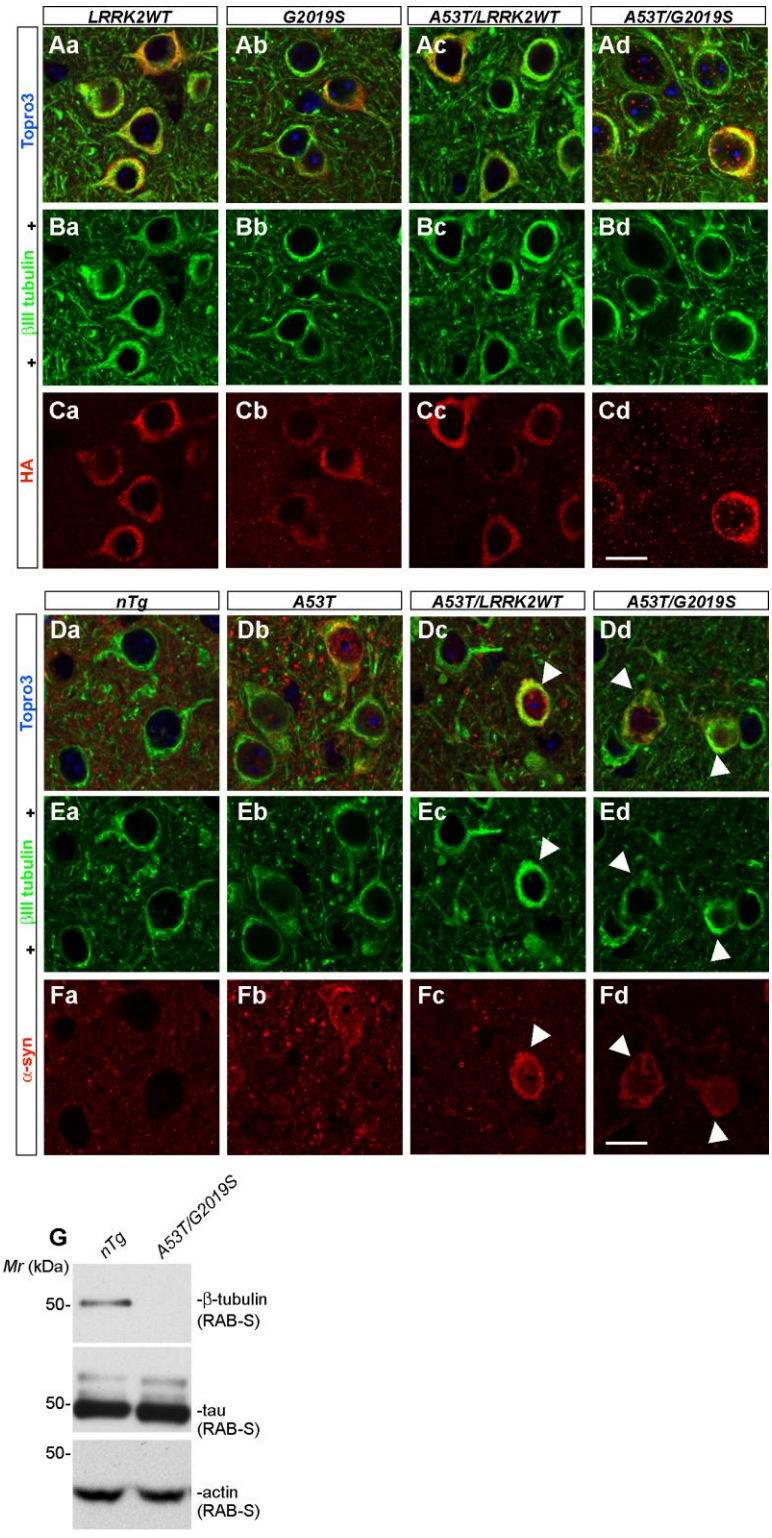
LRRK2WT
G2019S
A53T/LRRK2WT
A53T/G2019S
Aa
Ab
Ac
Ad
Ba
Bb
Bc
Bd
Ca
Cb
Cc
Cd
Topro3
+
βIII tubulin
+
HA
nTg
A53T
A53T/LRRK2WT
A53T/G2019S
Da
Db
Dc
Dd
Ea
Eb
Ec
Ed
Fa
Fb
Fc
Fd
Topro3
+
βIII tubulin
+
α-syn
G
nTg
A53T/G2019S
Mr (kDa)
50-
-β-tubulin
(RAB-S)
50-
-tau
(RAB-S)
50-
-actin
(RAB-S)

Figure S9

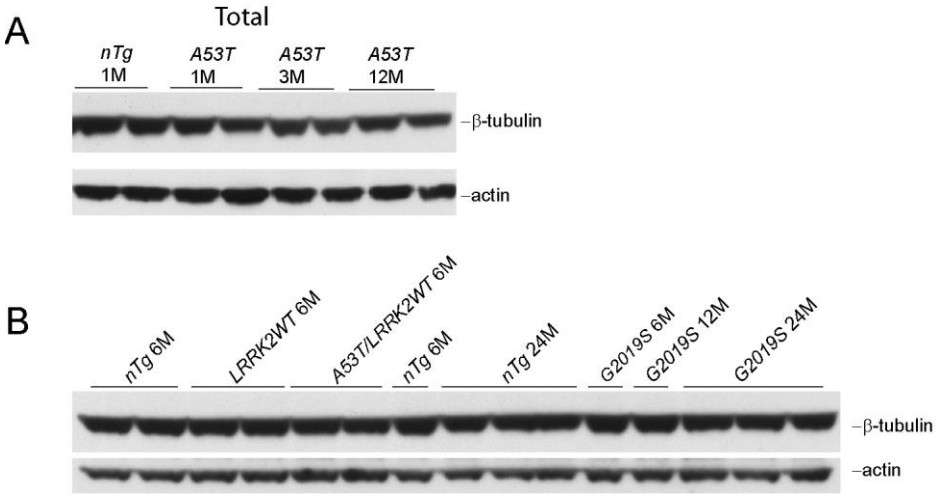

Figure S10

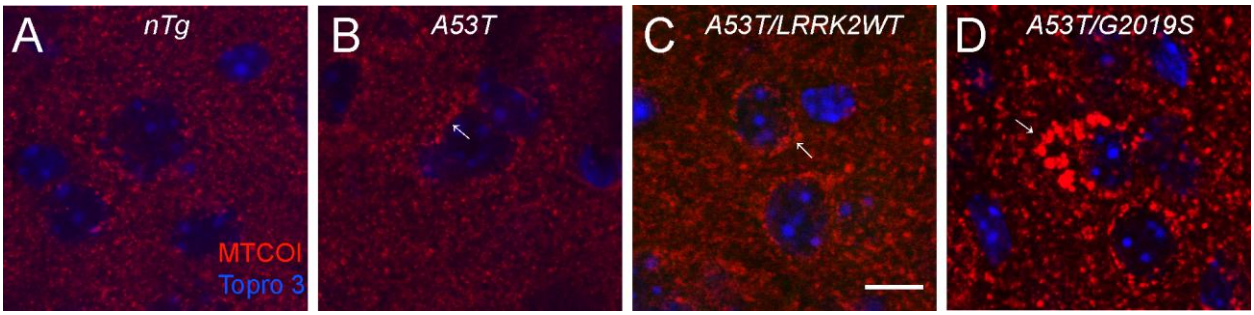

Figure S11

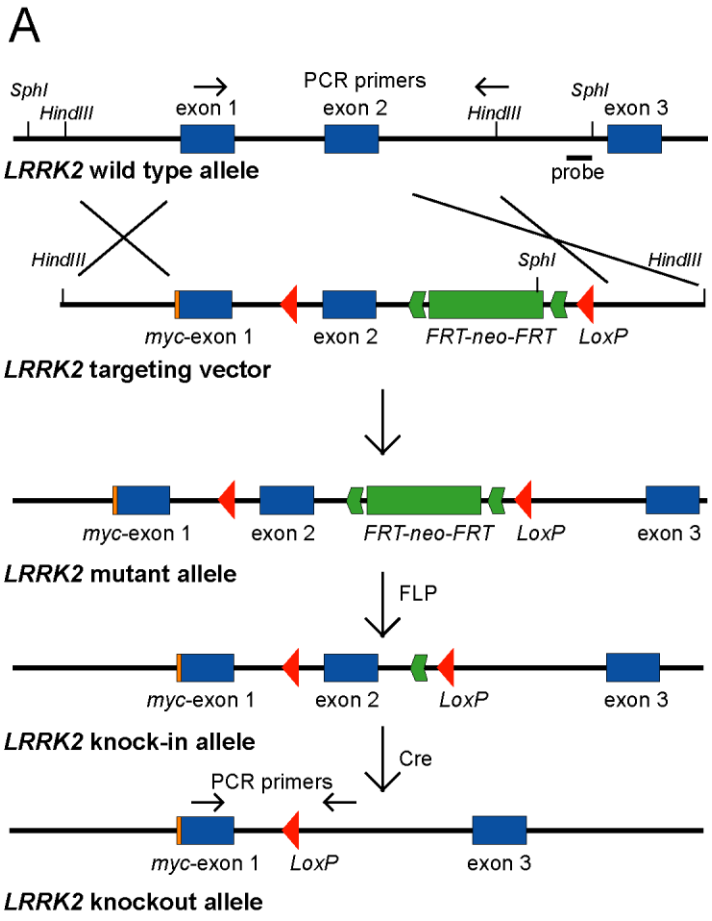
A
SphI
HindIII
exon 1
PCR primers
exon 2
HindIII
SphI
exon 3
LRRK2 wild type allele
probe
HindIII
SphI
HindIII
myc-exon 1
exon 2
FRT-neo-FRT
LoxP
LRRK2 targeting vector
myc-exon 1
exon 2
FRT-neo-FRT
LoxP
exon 3
LRRK2 mutant allele
FLP
myc-exon 1
exon 2
LoxP
exon 3
LRRK2 knock-in allele
Cre
PCR primers
myc-exon 1
LoxP
exon 3
LRRK2 knockout allele

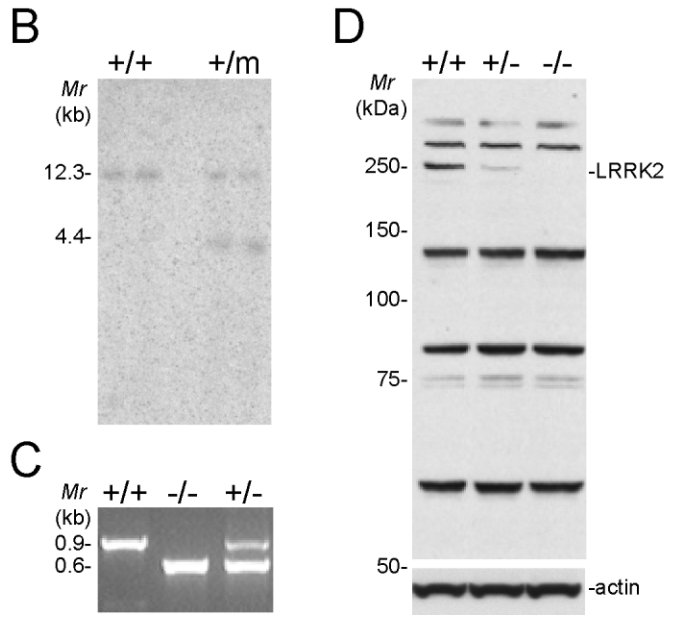
B
+/+
+/m
Mr
(kb)
12.3-
4.4-
C
Mr
+/+
-/-
+/-
(kb)
0.9-
0.6-
D
+/+
+/-
-/-
Mr
(kb)
250-
150-
100-
75-
50-
-LRRK2
-actin

Figure S12

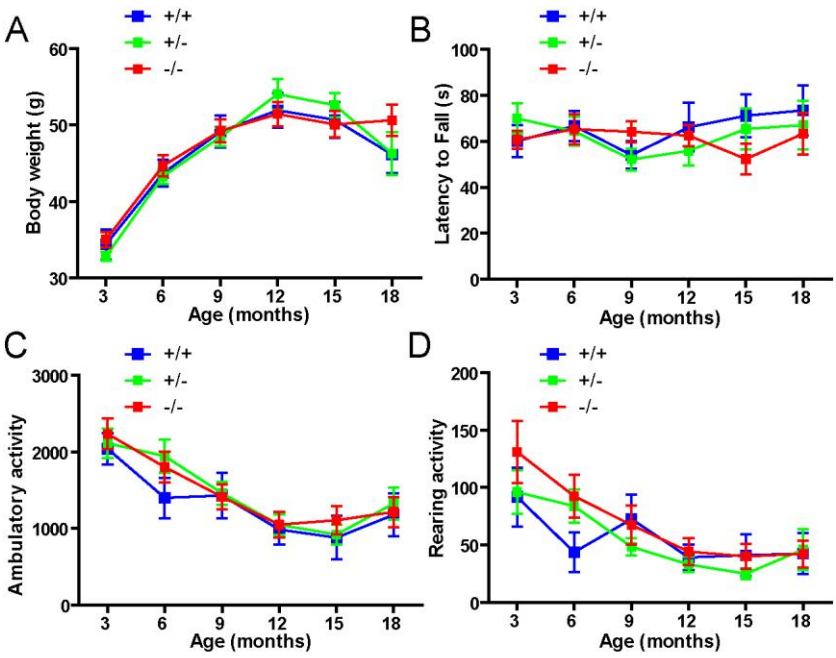
A
+/+
+/-
-/-
Body weight (g)
60
50
40
30
3
6
9
12
15
18
Age (months)
B
+/+
+/-
-/-
Latency to Fall (s)
100
80
60
40
20
0
3
6
9
12
15
18
Age (months)
C
+/+
+/-
-/-
Ambulatory activity
3000
2000
1000
0
3
6
9
12
15
18
Age (months)
D
+/+
+/-
-/-
Rearing activity
200
150
100
50
0
3
6
9
12
15
18
Age (months)

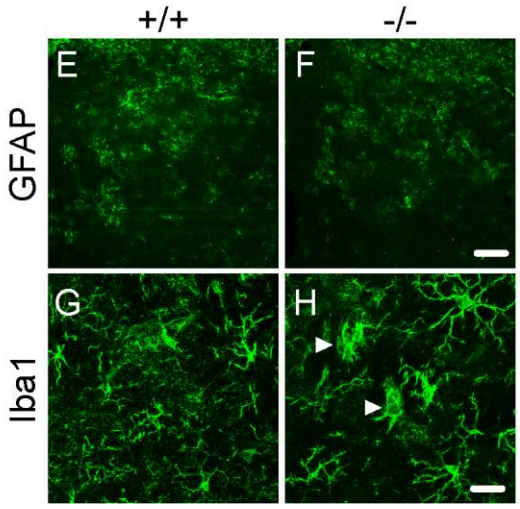
+/+
-/-
GFAP
Iba1
E
F
G
H

Figure S13

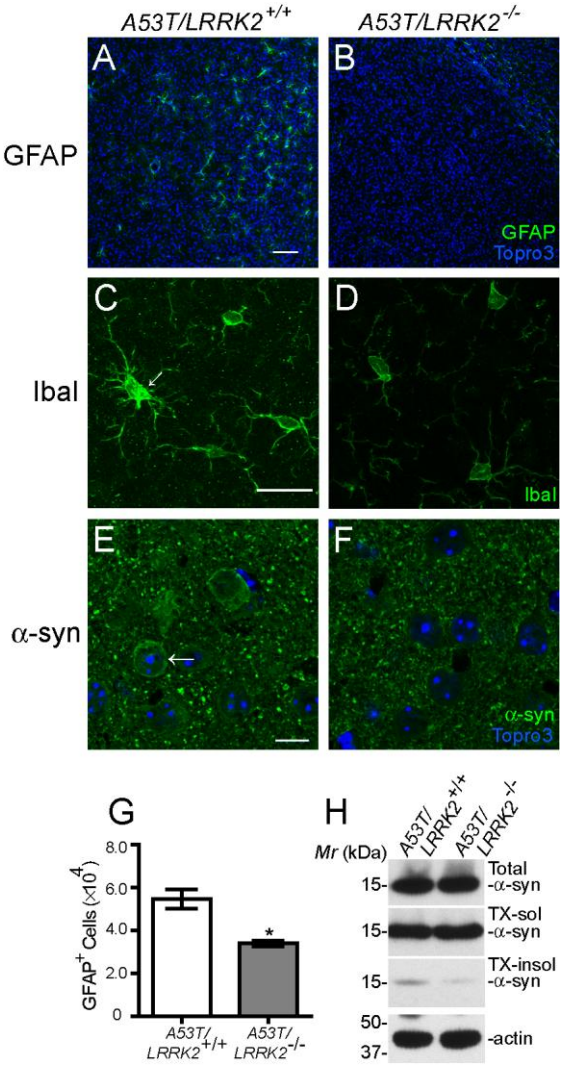
A53T/LRRK2+/+
A53T/LRRK2-/-
A
B
GFAP
GFAP
Topro3
C
D
Iba1
Iba1
E
F
α-syn
α-syn
Topro3
G
GFAP+ Cells (×10^4)
8.0
6.0
4.0
2.0
0
*
A53T/ LRRK2+/+
A53T/ LRRK2-/-
H
Mr (kDa)
A53T/ LRRK2+/+
A53T/ LRRK2-/-
15-
Total -α-syn
15-
TX-sol -α-syn
15-
TX-insol -α-syn
50-
37-
-actin